Effective-medium calculations for hydrogen in Ni, Pd, and Pt

Christensen, Ole Bøssing; Stoltze, Per; Jacobsen, Karsten Wedel; Nørskov, Jens Kehlet

Published in:
Physical Review B

Link to article, DOI:
10.1103/PhysRevB.41.12413

Publication date:
1990

Document Version
Publisher's PDF, also known as Version of record

Effective-medium calculations for hydrogen in Ni, Pd, and Pt

O. B. Christensen, P. Stoltze, K. W. Jacobsen, and J. K. Nørskov
Laboratory of Applied Physics, Technical University of Denmark, DK-2800 Lyngby, Denmark
(Received 28 December 1989)

The effective-medium theory is applied to a study of the energetics of the hydrides of Ni, Pd, and Pt, stressing the properties of PdH_θ for $0 \leq \theta \leq 1$. The calculated heat of solution and the heat of hydride formation for the three systems agree very well with experiment. We determine the favored structure for PdH_θ by calculating the total energy and lattice expansion of different configurations. Vibrational frequencies and diffusion barriers of H in Pd are also treated. A simple and transparent physical picture of the hydrogen-metal interaction is developed. From the calculated energetics we make a model calculation of the phase diagram of hydrogen in palladium in qualitative agreement with experiment. On this basis we propose a new explanation of the peculiarities of the Pd-H system.

I. INTRODUCTION

The large capacity of palladium to absorb hydrogen has made this system interesting from many points of view: fundamentally (quantum diffusion, hydride formation) as well as technologically (membranes, hydrogen storage, etc.).[1] It is therefore an interesting task to investigate the details of this particular system in the framework of numerical microscopic models.

In order to make comparative studies of configurations at varying hydrogen occupations, one has to consider a great deal of configurations and to include many atoms in the unit cell for each calculation. This makes it very hard to apply first-principles electronic-structure schemes to this problem.

It is well known that it is not possible to describe all total-energy properties of metals adequately by pair potentials. The elastic properties, for instance, are poorly described in such a model. In the present work, we want to describe deformations of a metallic lattice due to interstitial hydrogen. We therefore employ the effective-medium theory (EMT).[2] This model includes many-body interactions in an approximate manner but is still simple enough to permit calculations for a large number of configurations.

The EMT was originally applied to the calculation of the binding energies of small atoms like hydrogen in metals and on metal surfaces.[3,4] Previously,[3] hydrogen absorbed in metals, and in particular, its interaction with lattice defects, has been investigated in a simplified version of the EMT. The present work has applied an improved model of Ref. 5 enabling a description of the whole metal-impurity system instead of just the impurity. EMT has been successfully applied to a whole range of systems, including bulk properties of metals,[2] surface energies, relaxations and reconstructions,[2,6] chemisorption properties,[7] adsorption of molecular hydrogen on Ni and Cu surfaces,[5] and Monte Carlo and molecular-dynamics simulations of thermal expansion and melting.[8]

A similar model, the semiempirical embedded-atom method,[9] has been successfully applied for describing hydrogen-metal systems. Recently,[10] it has been used to model experimentally measured atomic forces in palladium hydride.

The quality of the application of EMT to the PdH_θ system is illustrated by a comparison of calculated quantities and trends to experiment. Heats of solution and of adsorption, as well as lattice constants and binding energies as functions of hydrogen occupation, have been calculated including the microscopic deformation of the perfect Pd lattice.

We also study the vibrational frequency and the diffusion barrier for hydrogen inside pure palladium.

The main purpose of this paper is to distill a very simple model for the interaction between hydrogen atoms inside a palladium crystal. From such a model we derive a phase diagram which agrees semiquantiatively with the experimentally measured one.

A preliminary account of some of these results has been published elsewhere.[11]

The paper is organized as follows. The effective-medium theory in the form applied here will be summarized. In Sec. III a number of calculations and their results are presented. Section IV deals with a simple model for the H-H interaction and the phase diagram derived from this. Finally, the main results will be discussed and the conclusions will be presented.

II. THE EFFECTIVE-MEDIUM THEORY

An atom embedded in a metallic system is to a large extent screened from its surroundings by the electron gas around it. Therefore, it is tempting to describe the system by approximating the local surroundings by a homogeneous electron gas. Thus the embedding energy of an atom is to a first approximation a function only of the electron density $\bar{n}$ contributed by the surroundings and independent of the composition of the host system.[4,9,12] For each kind of atom the total-energy change $\Delta E_{\rm hom}(\bar{n})$ associated with embedding the atom into a homogeneous electron gas of density $\bar{n}$ may be calculated once and for all within the local-density approximation.

The success of this relatively crude model in calculating trends and even absolute energies stems from the fact that errors in the electron density and in the one-electron potential entering the Kohn-Sham equations only give errors in the total energy to second order.[13,2]

Below we shall briefly review the various expressions and fundamental approximations used in EMT and in the calculations presented here. Details of the calculational method are deferred to Appendix A.

When an atom is embedded in a homogeneous electron gas it will induce a change in the electron density of some amount $\Delta n(|r|)$. Aiming at describing every atom in the system as embedded in a homogeneous gas consisting of the electron tails from all the surrounding atoms, we make the ansatz for the total electron density at every point in space

$$n(\mathbf{r})=\sum_i \Delta n_i(|\mathbf{r}-\mathbf{R}_i|) \tag{1}$$

summing over all atoms i. Now we calculate the density contributed by the surrounding $\bar{n}_i$ as $\langle \sum_{j\,(\neq i)} \Delta n_j(|\mathbf{R}_i-\mathbf{R}_j|)\rangle$, where the average is over a neutral sphere around atom i. We choose a neutral sphere because the effective medium is isotropic anyway so that there is no hope of doing better than that and because the neutrality of the sphere excludes long-range Madelung interactions between different spheres.

With this density ansatz the total energy may be written as[2]

$$E_{\rm tot}=\sum_i E_{c,i}(\bar{n}_i)+\Delta E_{\rm AS}+\Delta E_{\rm 1el}\ , \tag{2}$$

where the so-called cohesive function E_c is defined by

$$E_{c,i}(\bar{n})=E_{{\rm hom},i}(\bar{n})-\alpha_i(\bar{n})\bar{n}\ . \tag{3}$$

The first term in (3) is the energy of embedding atom i into a homogeneous electron gas. The second term is the electrostatic attraction inside the neutral sphere between the electron tails from the neighbors and the atom itself. Assuming a constant electron density $\bar{n}$ from the surroundings, this energy will look like

$$-\int\int_{\text{neutral sphere}} d\mathbf{r}\,d\mathbf{r}'\frac{\bar{n}(\mathbf{r})\Delta n(\mathbf{r}')}{|\mathbf{r}-\mathbf{r}'|} =\bar{n}\int_{\text{neutral sphere}} d\mathbf{r}\,\Delta\Phi(r)=:-\alpha\bar{n}\ , \tag{4}$$

where $\Delta\Phi$ is the electrostatic potential induced by the atom. This electrostatic attraction is not included in $\Delta E_{\rm hom}$ because the electrostatic interaction between a homogeneous system with a compensating positive background and a neutral atom is zero.

The most important contribution to the first correction term in (2) is electrostatic. Let us define the overlap function $\mathcal{O}(\mathbf{r})$ as $n-1$ at points in space inside n atomic spheres. Then we have simply[2]

$$\Delta E_{\rm AS}=-\int d\mathbf{r}\,\mathcal{O}(\mathbf{r})n(\mathbf{r})\Phi(\mathbf{r})\ , \tag{5}$$

Φ being the total electrostatic potential. This term is dominated by the repulsive interaction between different nuclei when neutral spheres overlap so that the screening is not complete. The details of how $\Delta E_{\rm AS}^{\rm H_xPd}$ is evaluated can be found in Appendix A.

The second correction term $\Delta E_{\rm 1el}$ describes the difference in Kohn-Sham one-electron energy between the atom embedded in the real metal and the atom embedded in a homogeneous electron gas. Denoting the change in density of states by embedding atom i into the two systems by $\Delta n_i^{\rm met}(\varepsilon)$ and $\Delta n_i(\varepsilon)$, respectively, we have

$$\Delta E_{\rm 1el}=\sum_i\left[\int_{-\infty}^{\varepsilon_F^{\rm met}} d\varepsilon\,\varepsilon\Delta n_i^{\rm met}(\varepsilon)-\int_{-\infty}^{\varepsilon_F} d\varepsilon\,\varepsilon\Delta n_i(\varepsilon)\right]\ , \tag{6}$$

where $\varepsilon_F^{\rm met}$ and ε_F are the two Fermi energies.

This correction term is only significant in the case of transition metals. In calculating the two densities of states the same atomic potential should be used. It can be calculated within the Newns-Anderson model.[2,5,14] In the present calculations we only include the interaction between the Pd d band and the H s band. It turns out to vary very little with the configuration.

The interaction between two hydrogen atoms deviates from the term $2E_c(\Delta n(|\mathbf{r}_{\rm HH}|))$, where one hydrogen sees the other as a jellium. We define the difference

$$\delta(r,n^{\rm background})=E_{\rm H_2}^{\rm exact}(r,n^{\rm background})-2E_c(\Delta n(r))\ . \tag{7}$$

The first term is the total energy of two hydrogen atoms separated by r in a jellium of density $n^{\rm background}$ equal to the density contributed by all other atoms in the system. The function δ has been calculated[5,15] in the local density approximation and turns out to be effectively independent of the density.[5]

III. RESULTS

All calculations below have been made in the following way: The hydrogen is placed in the required site in the perfect, unrelaxed metal lattice. Then the size of the unit cell, as well as the position of each atom, is varied according to the Direction Set Method[16] to find a relaxed local minimum. We apply periodic boundary conditions and measure energies relative to metallic Pd and free H_2. Superscripts on energy terms and EMT constants denote the kinds of atoms on which they depend.

A. Heats of solution and hydride formation

The heat of solution of H in the three metals Ni, Pd, and Pt was calculated by placing one H in a supercell consisting of $3\times3\times3$ primitive Pd cells (27 Pd atoms). The results are shown in Fig. 1. The heat of absorption at concentration $\theta=1$ (hydrogen atoms per palladium atom) comes from a calculation with one H and one Pd atom in the cell (Fig. 2). Experimental results are from Ref. 17.

In the EMT picture, the decisive property expected to cause the trend in the heat of solution is the value of the electron density in the interstitial site determining the value of the cohesive function E_c. This function has a single minimum. In all cases considered here, the hydrogen atom is embedded in a much higher electron density

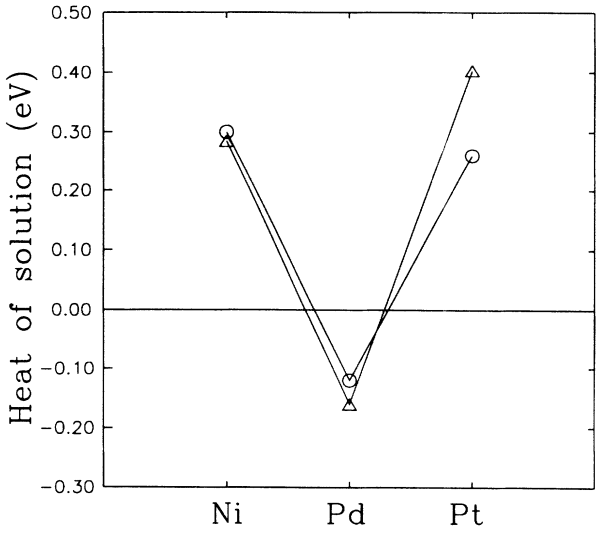

FIG. 1. Heat of solution. Total electronic energy of $3\times3\times3$ metal unit cells and one hydrogen in an octahedral site measured relative to pure metal and free H_2. ○, calculated results; △, experiment (Ref. 17). In the case of Pd thermal energy should reduce the calculated energy by 77 meV.

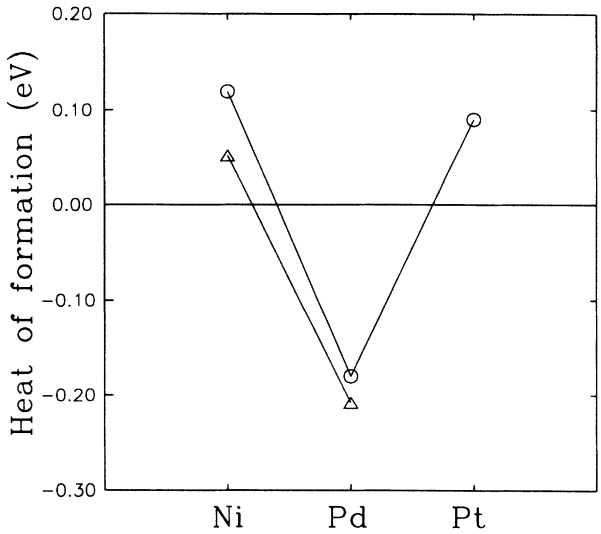

FIG. 2. Heat of absorption. Total energy of metal monohydride primitive cell relative to pure metal and free H_2. ○, calculated results; △, experiment (Ref. 17).

than the optimal one. Thus, the lower the interstitial electron density of the metal, the lower the value of the cohesive function E_c^H. For all systems considered, the hydrogen atoms prefer the octahedral to the tetrahedral sites in accordance with this picture. The energy difference between nickel and palladium is driven by the difference in interstitial electron density as the lattice constant of Ni is much smaller than that of Pd. As far as Pt is concerned, the matter is a bit more complex: the interstitial density before relaxation gives rise to a difference in E_c of only 160 meV. The main difference between Pd and Pt is that the latter is much harder. This is reflected in the fact that the EMT parameters η and α are larger in the case of Pt. Therefore the presence of H does not reduce the neutral radii as much, thus not making $\Delta E_{AS}^{Pt,Pt}$ as negative as in the case of Pd.

In the results of Figs. 1 and 2 some of the contributions to the total energy have not been included. Our calculations do not include the thermal energies or the zero-point energies of vibration of either the PdH_θ system or of the H_2 molecule to which it is compared, whereas these terms are part of the experimental energies plotted. These terms may be estimated as follows:

$$E_{\text{thermal}}(\text{free } H_2)=\tfrac{5}{2}k_BT+k_BT+\tfrac{1}{2}\hbar\omega_{\text{H-H}} , \quad (8)$$

where the three terms represent translational thermal energy, rotational thermal energy, and vibrational zero-point energy of the H_2 molecule, respectively. For the palladium hydride system we get

$$E_{\text{thermal}}(\text{H in Pd})=3k_BT+\tfrac{3}{2}\hbar\omega_0+\tfrac{1}{2}k_BT , \quad (9)$$

where the first term is the thermal and the second is the zero-point energy of the hydrogen vibration, the last has to do with the work of compressing the hydrogen into the bulk metal.

At $T=300$ K, $\hbar\omega_{\text{H-H}}=540$ meV (from our calculation), $\hbar\omega_0=68.5$ meV (from Ref. 1) we get

$$\tfrac{1}{2}E_{\text{thermal}}(\text{free } H_2)-E_{\text{thermal}}(\text{H in Pd})$$
$$=180 \text{ meV}-103 \text{ meV}=77 \text{ meV} . \quad (10)$$

This term is expected to be of the same order of magnitude for the other two metals considered. The neglect of these correction terms is thus well justified, when the approximate nature of the calculation is taken into account.

The numerical agreement apparent from the figures is probably fortuitous, but the trends are accurately described, thus giving reason to believe that we have a realistic picture of the essential physics of the hydrogen-metal system.

B. Expansion and stability of palladium hydride

In a $3\times3\times3$ supercell we have placed hydrogen atoms randomly in octahedral sites. The binding energy per H atom relative to molecular H_2 is shown in Fig. 3. In Fig. 4 calculations with more than one hydrogen in a primitive Pd unit cell is included. One contribution to the large jump at $\theta=1$ is that the Pd d band becomes filled, thus stopping the bond formation between Pd d and H s orbitals. The main reason is, however, that the hydrogen atoms are now forced to occupy tetrahedral sites instead of octahedral. At $\theta=4$ the octahedral and the two tetrahedral sites per Pd atom fill, and the last H atom is found around the octahedral site forming a quasimolecule with a H-H distance of 1.89 bohr; large compared to the value of 1.4 bohr for free H_2.

A systematic calculation was performed in a $2\times2\times2$ supercell, where all possible distributions of hydrogen in octahedral sites were investigated. Figure 5 shows the minimum-energy states for each possible occupation of H in this cell—the result for one H among 27 Pd atoms is plotted as well, as it is also a minimum-energy

configuration. The lattice constants are shown in Fig. 6 and compared with experimental results[18] for the β phase. The values agree at $\theta=0$ because of the fit of s_0^{Pd}. The fact that the expansion of the lattice with increasing hydrogen occupation is slightly overestimated suggests that the H-Pd repulsion term $\Delta E_{\mathrm{AS}}^{\mathrm{H,Pd}}$ is too hard. This is not unexpected since the calculation includes repulsive contributions to this quantity but neglects attractive ones. This fact will be important for the treatment of diffusion below.

The energy curve of Fig. 5 is very interesting. Until an occupation of about one-half, it seems to agree with the linear prediction of a simple picture with an effective concentration-independent pairwise attraction between hydrogen atoms ($E_{\mathrm{tot}} \sim \alpha\theta - \beta\theta^2 \Longrightarrow E_i \sim \alpha - \beta\theta$).[19] Above $\theta=0.5$, however, the calculated energy per atom is almost constant. As a consequence, until an occupation of one-half, hydrogen atoms will attract each other. But when $\theta=0.5$ has been reached this is no longer the case and the entropy will prevent the occupation from increasing further. This effect may explain the experimentally observed maximum hydrogen occupation of about 0.6. It is investigated in the following section.

To determine the reason for the shape of the energy curve, in Fig. 7 we show the different EMT energy contributions per hydrogen atom relative to the value at $\theta=0.125$ with one hydrogen atom in the cell. The driving attractive force between hydrogen atoms is obviously E_c^{H}. As the hydrogen atoms expand the palladium lattice, their embedding density and thus E_c^{H} decreases. The repulsive behavior of $\Delta E_{\mathrm{AS}}^{\mathrm{Pd,Pd}}$ is explained as follows. When the hydrogen expands the lattice the mutual overlap between Pd atoms decreases making $\Delta E_{\mathrm{AS}}^{\mathrm{Pd,Pd}}$ negative. The absolute value increases with θ, but not proportionally, so that the value per hydrogen atom decreases. In other words, when the hydrogen atoms screen the different palladium nuclei effectively no more electrostatic energy is gained by adding even more H. This explains the kink in E at $\theta \simeq 0.5$.

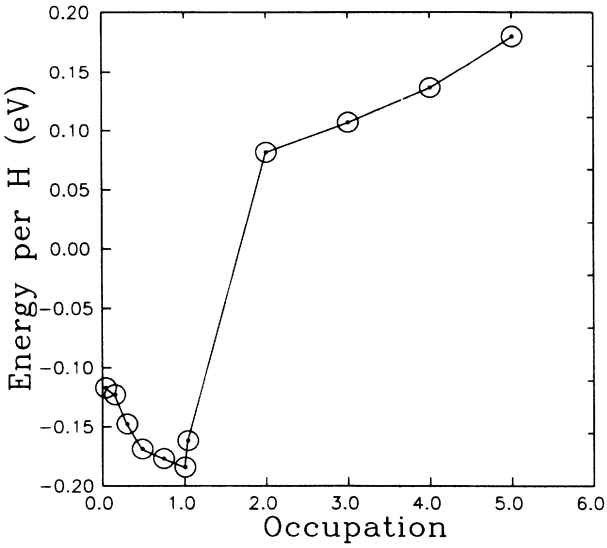

FIG. 4. Binding energy of H. For $\theta<1$ calculated in a $3\times3\times3$ Pd unit cell, for $\theta\geq1$ in one Pd unit cell.

In order to determine the energy cost of getting two hydrogen atoms close together a 28th H atom was put inside a $3\times3\times3$ PdH lattice and moved between a tetrahedral site and one already occupied octahedral site. Both an unrelaxed calculation and a fully relaxed were made, see Fig. 8. In the latter, the only fixed coordinate was the distance between two of the hydrogen atoms.

Recent first-principles calculations[20] at $\theta=\frac{1}{4},\frac{1}{2},1,2,$ and 3 confirm most of our conclusions as regards properties at physical values of θ. The authors find the same minimum-energy configurations for different values of θ except in the case of PdH_2, where they find that the hydrogen atoms occupy two tetrahedral sites instead of one octahedral and two tetrahedral sites. The shape of the energy-occupation curve is similar to the one calculated

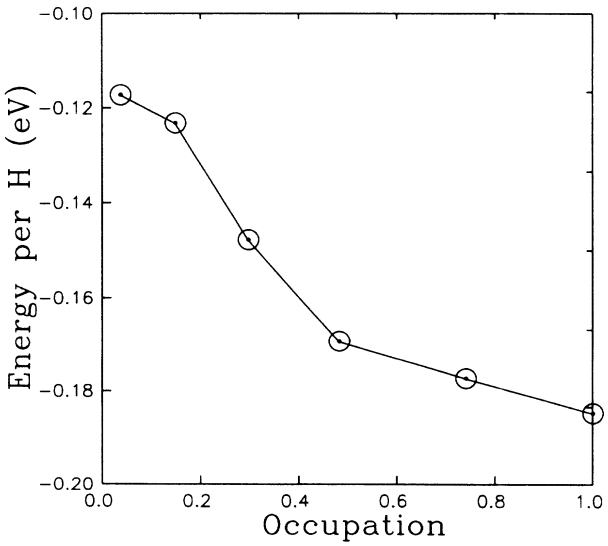

FIG. 3. Binding energy per H in a $3\times3\times3$ Pd unit cell with θ H atoms per Pd.

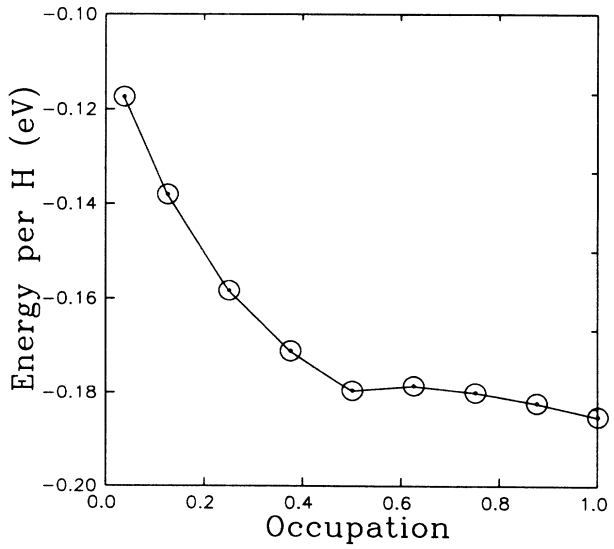

FIG. 5. Energy minimized over configurations of H in a $2\times2\times2$ unit cell with θ H atoms per Pd. Also the value for one H in a $3\times3\times3$ Pd cell is plotted.

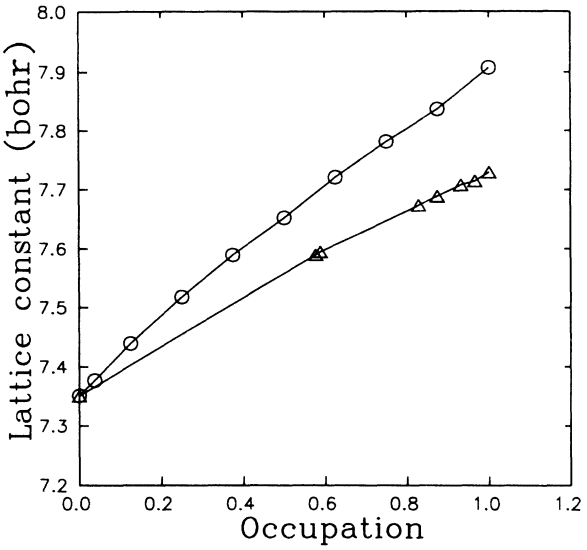

FIG. 6. Lattice constant relative to pure Pd. ○, calculations, like Fig. 5; △, experimental results at $T=77$ K (Ref. 18).

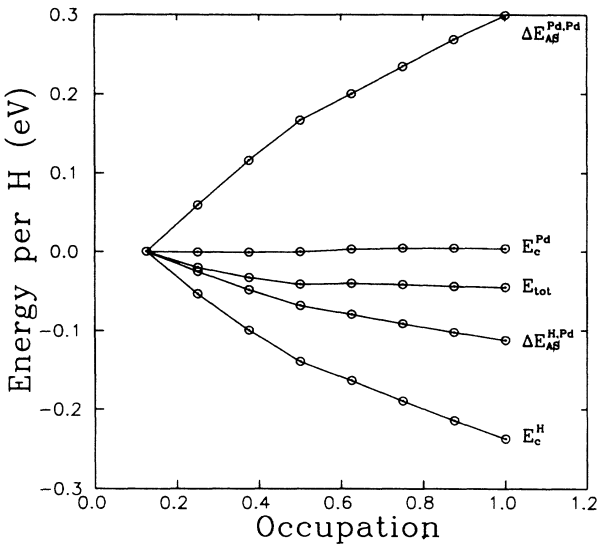

FIG. 7. EMT contributions to the total energy of Fig. 5 measured relative to $\theta=\frac{1}{8}$.

by us. The calculated lattice constant as a function of θ is in somewhat better agreement with experiment than ours. A calculation of energy as a function of the hydrogen-hydrogen distance in a PdH_2 cell with an octahedrally centered H_2 quasimolecule along the (111) direction gives qualitative but not quantitative agreement with a similar calculation by us. The apparent failure for our model to adequately describe $\theta>1$ is probably due to the very crude description of bonding between palladium d and hydrogen s orbitals.

C. Diffusion

Hydrogen diffusion in palladium between two octahedral sites must go via a tetrahedral site. In Fig. 9 results are shown where one hydrogen atom is moved in a $3\times3\times3$ unit cell from an octahedral to a tetrahedral site. In the unrelaxed calculation all Pd atoms are kept fixed. In the next one the six-nearest neighbors are allowed to move and in the final one the eight next-nearest neighbors may relax also—of course we have to keep some Pd fixed to avoid just translating the whole lattice along with the hydrogen atom when minimizing.

The relaxation is extremely important for the size of the diffusion barrier, but it is found to be considerably higher than the experimental value of 230 meV (Ref. 21) even in the most relaxed case, where it is 743 meV. This is in accordance with the previously mentioned fact that the hydrogen-metal interaction term $\Delta E_{AS}^{H,Pd}$ is too repulsive. The same is seen in a calculation of the vibrational frequency of H at the octahedral site, which is calculated to $\omega_0=126$ meV, whereas the experimentally measured one is $\omega_0=68.5$ meV. To get a more realistic description of the system at the diffusion barrier we make a one-parameter fit of $\Delta E_{AS}^{H,Pd}$ reproducing the experimental vibrational frequency at the octahedral site keeping the total energy in this configuration the same as before the fitting. The error in the way we calculate $\Delta E_{AS}^{H,Pd}$ is least serious at the interstitial sites when $\Delta E_{AS}^{H,Pd}$ is small (it only shows up as a small error in the expansion) but becomes more serious when the hydrogen atom is moved closer to the palladium atoms. A further description of the fitting procedure can be found in Appendix B.

With the fitted $\Delta E_{AS}^{H,Pd}$ the fully relaxed (nearest-neighbors and next-nearest-neighbors) energy curve looks as in Fig. 10. As the hybridization at the top of the barrier turns out be different from the values at the local minima, we have included a calculation of ΔE_{1el} at each point.

The fitting procedure that only referred to local

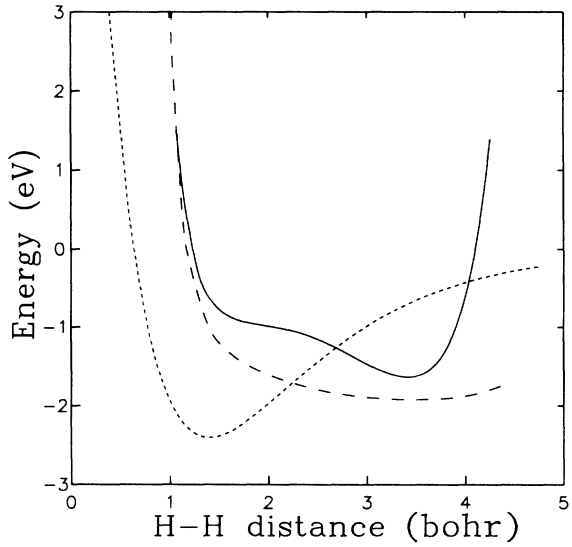

FIG. 8. Energy relative to pure Pd and *atomic* H of $3\times3\times3$ PdH with one extra H moved between an occupied octahedral site and a tetrahedral site. Solid curve: no relaxation of lattice relative to PdH. Long dashed curve: only one H-H distance and cell size kept fixed, all other coordinates relaxed. Short dashed curve: for comparison, Morse potential of H_2 molecule.

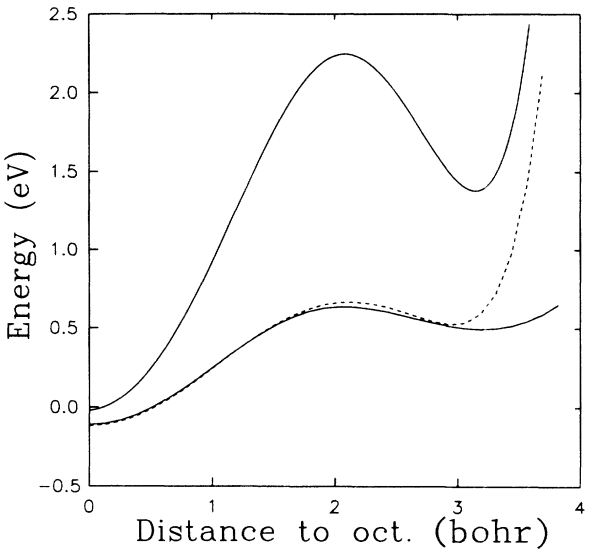

FIG. 9. Total energy moving one H in 3×3×3 Pd cell from the octahedral to tetrahedral site. Upper solid curve: no relaxation. Dashed curve: six-nearest neighbors to octahedral site relaxed. Lower solid curve: also eight next-nearest neighbors relaxed.

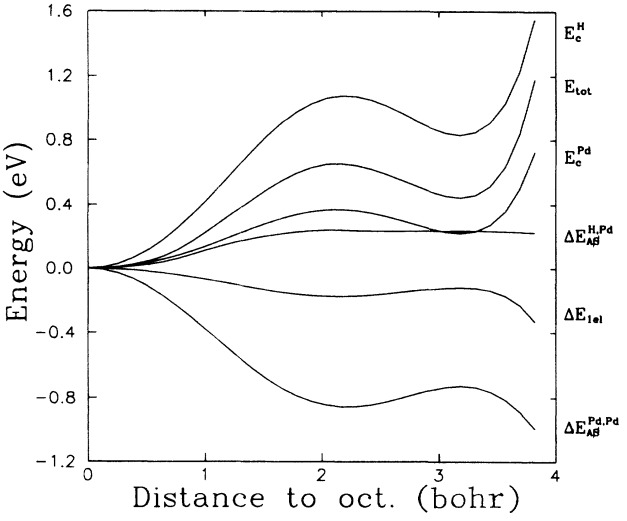

FIG. 11. EMT energy contributions moving one H from the octahedral to a tetrahedral site in 3×3×3 Pd lattice without relaxation. All terms measured relative to the octahedral site.

features of the ground state gives rise to a much improved diffusion barrier. The barrier height is 313 meV, which is only 83 meV away from the experimental value. Note that zero-point energies and thermal energies $k_B T \sim 30$ meV have been ignored in the comparison to experiment.

When comparing the different energy contributions we look at the unrelaxed case first. From Fig. 11 it is seen that the important term is E_c^H. The energy simply follows the contour of embedding electron density. The more effective screening of Pd atoms in the vicinity of H is mirrored by the shape of $\Delta E_{AS}^{Pd,Pd}$. This term reduces the effect of E_c^H but does not cancel it completely. In the relaxed case (Fig. 12) the energy distribution among the different terms does not vary qualitatively. It turns out that all magnitudes are reduced by about the same amount. At the high-symmetry tetrahedral site there is a difference because of an efficient relaxation of several Pd atoms, decreasing the embedding density of H but not pushing any two Pd atoms very close together.

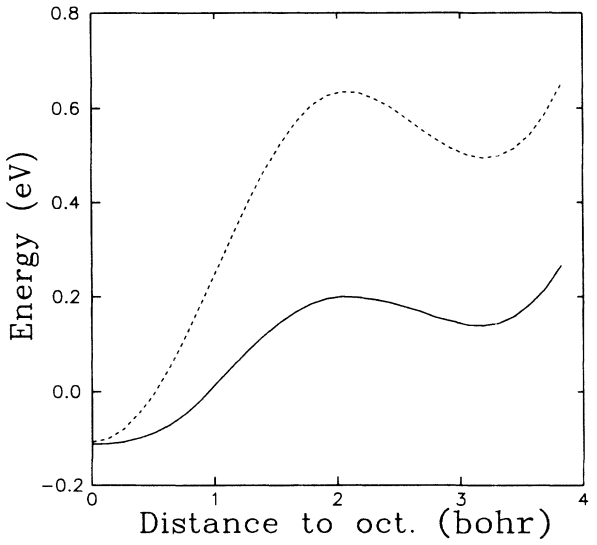

FIG. 10. Relaxed motion of H from the octahedral to tetrahedral site in 3×3×3 Pd cell. Dashed curve: original parameters. Solid curve: fitted $V^{H,Pd}$ and ϕ_R.

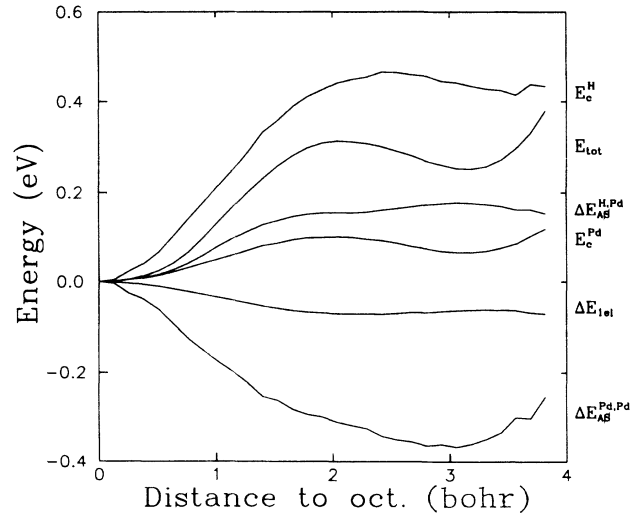

FIG. 12. EMT energy contributions moving one H from the octahedral to a tetrahedral site in 3×3×3 Pd lattice relaxing 14 nearest Pd atoms. All terms measured relative to the octahedral site.

IV. THERMODYNAMIC MODEL

In the present section we will illustrate the results of the previous sections in an approximate calculation of the phase diagram for the PdH_θ system. The thermodynamic model to be developed in the following is based on placing a number of hydrogen atoms on an fcc lattice, the hydrogen atoms vibrate around their perfect lattice sites in an uncorrelated fashion and an effective field mediates a hydrogen-hydrogen interaction.

For the hydrogen atoms we will write the grand canonical partition function

$$\Xi(T,\mu)=\sum_n \sum_{\text{conf}} \exp\left[\frac{\mu n - W}{k_B T}\right] z^n , \tag{11}$$

where n is the number of H atoms distributed on N sites. In this equation the second summation extends over all configurations of the atoms, W is the total interaction energy for the configuration. The summation over collective degrees of freedom is thus performed by the summation over configurations using the interaction energy W in the calculation of the statistical weight. The partition function for an atom in the absence of interactions is z. For this we use an Einstein model with vibration quantum $\hbar\omega=68.5$ meV:

$$z=\frac{\exp\left[-\frac{3\hbar\omega}{2k_B T}\right]}{\left[1-\exp\left[-\frac{\hbar\omega}{k_B T}\right]\right]^3}\exp\left[-\frac{\varepsilon_0}{k_B T}\right] . \tag{12}$$

We adopt a mean-field approximation similar to the Bragg-Williams approximation in writing

$$\sum_{\text{conf}} \exp\left[-\frac{W}{k_B T}\right]=\frac{N!}{n!(N-n)!}\exp\left[-\frac{nw}{k_B T}\right] , \tag{13}$$

where we allow the interaction energy w to depend on the overall occupation, $\theta=n/N$. Using Fig. 5 we find $\varepsilon_0=0.075$ meV,

$$w=\varepsilon_1(1-\theta)^\alpha , \tag{14}$$

with $\varepsilon_1=0.075$ eV and $\alpha=3.67$ to be an adequate description.

We derive an expression for the chemical potential by retaining the dominating term in (11),

$$\mu_H=\mu_0+k_B T\ln\left[\frac{\theta}{1-\theta}\right]+w(\theta)+\frac{dw}{d\theta}\theta ,$$
$$\mu_0=-k_B T\ln(z) . \tag{15}$$

We note that this procedure corresponds to the suppression of the fluctuations for θ. In the thermodynamic limit, this procedure is exact for the thermodynamic data considered in the following.

The quantity $\mu(\theta)$ may display $(\partial\mu/\partial\theta)<0$ for suitable choices of θ and temperature. This indicates a thermodynamic instability and is a reflection of a first-order phase transition in the mean-field treatment. The correct behavior is found by substituting a discontinuity in $\theta(\mu)$ for the unstable part of the curve.

We treat the gas phase as ideal

$$z_{H_2}=\left[\frac{2\pi m k_B T}{h^2}\right]^{3/2}\left[\frac{k_B T}{p}\right]\left[\frac{k_B T}{2B}\right]\times\frac{\exp\left[-\frac{\hbar\omega}{2k_B T}\right]}{1-\exp\left[-\frac{\hbar\omega}{k_B T}\right]}\exp\left[-\frac{\varepsilon_{H_2}}{k_B T}\right]$$
$$\mu_{H_2}=-k_B T\ln(z) \tag{16}$$

where m is the mass of the molecule, p is pressure, B is the rotational quantum, $\hbar\omega$ is the vibrational quantum for H-H stretch and ε_{H_2} is the electronic ground-state energy for H_2. The calculations in Fig. 5 show the electronic energy of H inside Pd relative to $H_2(g)$. The convention adopted in the calculations of electronic energies corresponds to defining $\varepsilon_{H_2}=0$ for $H_2(g)$ at $T=0$.

The chemical equilibrium condition is

$$2\mu_{H_*}=\mu_{H_2} , \tag{17}$$

where μ_{H_*} is the chemical potential of a hydrogen atom inside the palladium lattice. We treat this equation numerically, using the above expressions for the chemical potential.

The calculated phase diagram based on our simple model is compared to the experimental one in Fig. 13. The agreement is surprisingly good, considering the simplicity of our thermodynamic model and the crudeness of the energy calculation. In the calculated phase diagram a miscibility gap arises between the α phase (low θ) and the β phase (high θ). The existence of the α phase is purely an entropy effect as this phase does not exist at $T=0$. The β phase extends over a rather large composition interval from $\theta\sim0.5$ to $\theta=1$ at low temperature. The curvature of the interaction energy $\omega(\theta)$ causes an asymmetry in the position of the miscibility gap. If $w(\theta)$ had been linear, the miscibility gap would have been placed symmetrically around $\theta=\frac{1}{2}$ in the phase diagram. The important experimental observation described by the model is the fact that we find a miscibility gap at $T=0$ at a hydrogen concentration less than 1. In our model a further filling of the lattice is energetically possible, although the equilibrium pressure rapidly increases for $\theta>\frac{1}{2}$ for entropy reasons. While the properties of PdH_θ change discontinuously at the transition from the α to the β phase, the properties change continuously during further filling of the lattice in the β phase.

By fitting Eq. (14) to the experimental phase diagram, we have found that the experimental miscibility gap is well reproduced by the values $\varepsilon_1=0.103$ eV and $\alpha=1.60$. The topology of the miscibility gap is independent of ε_0. Comparing the parameters found from the experimental phase diagram to the calculated parameters (Fig. 14) we find that the overall agreement is good, the major

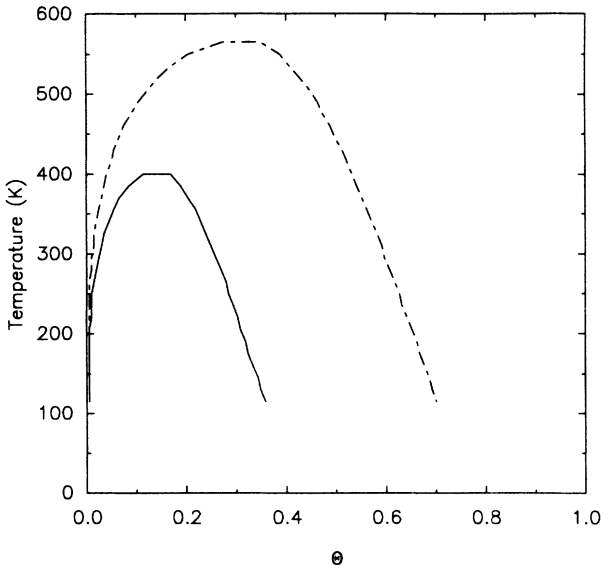

FIG. 13. Experimental phase diagram (dashed curve) compared to a phase diagram (solid curve) calculated from the data in Fig. 5, where the minimum interaction energy for each value of θ is used for w.

difference is that the parameters derived from experiment show less curvature for $\varepsilon(\theta)$. The differences in curvature is not unexpected from the small size of the system used in the computations. The differences in curvature is reflected in the differences in the width of the miscibility gap.

To reiterate, the hydrogen atoms expand the Pd lattice. The expansion at one site facilitates the expansion at neighbor sites. This leads to an effective H-H attraction. The cooperation levels off when about half of the sites are filled. It is this effect that shifts the position of the miscibility gap with respect to the line $\theta=\frac{1}{2}$ and gives rise to miscibility gap at $T=0$ of about 0.5. Our model is in contrast to earlier descriptions,[1,19] where the position of the gap is attributed to a steep increase of the Fermi energy derivative $dE_F/d\theta$ at the concentration where the palladium d band has been filled with electrons contributed by the hydrogen. Our calculation of $\Delta E_{\rm el}$ assumes a fixed E_F and thus does not include the mentioned mechanism. It should be mentioned that recent band-structure calculations[22] predict that the Pd d band lacks about 1.4 electrons per Pd atom to be completely filled. This is in contrast to earlier calculations, where the value was closer to the ~ 0.6 contributed by hydrogen at the lower limit of stability for the β phase at room temperature.

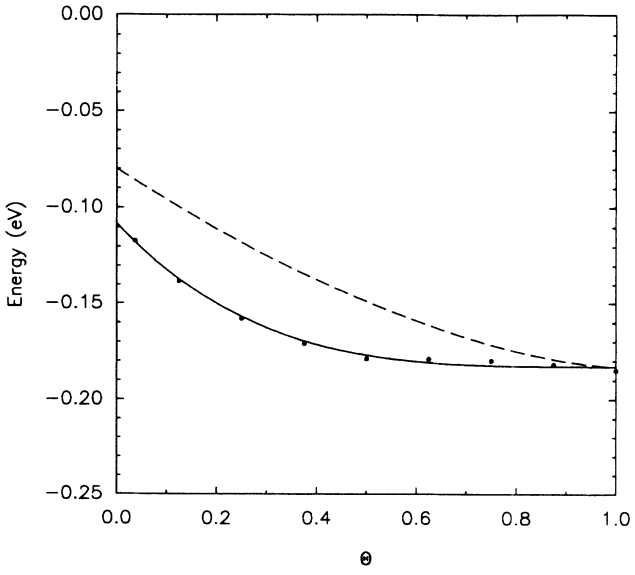

FIG. 14. The energy from (14) calculated from the experimental phase diagram (dashed curve) compared to the minimum interaction energies from Fig. 5 (solid curve).

V. SUMMARY

The purpose of the present paper has been threefold. First, we have devised a potential for the interaction of hydrogen with palladium. The functional form of the potential is derived from density-functional theory using effective-medium theory. The parameters entering are determined from independent calculations or by comparing to experimentally determined properties of the bulk metal. The potential gives a quantitative description of heats of solution and heats of hydride formation of Pd and of the neighboring systems of Ni and Pt. It also gives a good description of the expansion of the Pd lattice due to the hydrogen. If we allow one parameter to be fixed to give a good vibrational frequency for interstitial hydrogen, we can also give a semiquantitative description of the diffusion. All details of the potential are listed, and it is to be expected that it can be useful for more detailed studies of, for instance, the quantum diffusion of hydrogen in palladium.

Second, the model calculations have provided a simple physical picture of the hydrogen-palladium interaction. As proposed earlier,[3] it is found that most of the interaction can be understood by thinking of the hydrogen energy inside the metal as given by a function of the metal electron density at the site of the hydrogen. Further details have been added to this picture having to do with deformations of the palladium lattice due to the hydrogen atoms.

Third, the calculations have given an effective H-H interaction in Pd which depends crucially on the density of hydrogen in the lattice. Up until the lattice is about half-filled the interaction is attractive, the attraction being mediated by the distortions of the metal lattice as in ordinary continuum theories of the H-H interactions in metals. Beyond half-filling the interaction levels off, and the attraction goes to zero as the degree of filling approaches 1. On this basis we make a model calculation of the PdH_θ phase diagram, and show that such a behavior of the effective H-H interaction can be responsible for the observations that the hydride is stable from a filling θ of the H sites of about 0.6 and that beyond $\theta \simeq 0.6$ the hydride changes properties continuously as more hydrogen is added. This description stands in contrast to earlier

models, where concentrations above this value are excluded because of filling of the palladium d band.

APPENDIX A: CALCULATIONAL DETAILS

Here the practical computational procedure of the present calculations will be presented. See also Ref. 2. Let us consider a system consisting of a slightly distorted fcc lattice of palladium and some interstitial hydrogen atoms. The expressions are also valid in the case of Ni or Pt.

The cohesive energy function E_c is expanded to third order around its minimum

$$E_c = E_0 + E_2 \left[\frac{\bar{n}}{n_0} - 1 \right]^2 + E_3 \left[\frac{\bar{n}}{n_0} - 1 \right]^3 . \tag{A1}$$

The constants E_0, E_2, E_3, and n_0 are extracted from local-density approximation (LDA) calculations of the atom in jellium.

From the same calculations one finds to a good approximation the relationship

$$\bar{n}(s) = n_0 e^{-\eta(s-s_0)} \tag{A2}$$

between the embedding density and the neutral radius s of an atom. Also the average $\Delta\bar{n}(r,s)$ of Δn over a sphere of radius s positioned at a distance r from the atom is assumed exponential in s and r. Assuming that the embedding density of one atom in a fcc lattice only comes from the nearest neighbors we get

$$\Delta\bar{n}(r,s) = \frac{n_0}{12} e^{\eta_1(s-s_0) - \eta_2(r-\beta s_0)} , \tag{A3}$$

where $\beta = (16\pi/3)^{1/3}/\sqrt{2}$ is the ratio between the nearest-neighbor distance and the Wigner-Seitz radius in an fcc lattice and where

$$\eta = \beta\eta_2 - \eta_1 . \tag{A4}$$

Let us now consider the atomic-sphere correction $\Delta E_{\rm AS}^{\rm H,Pd}$. In the case of interaction between identical atoms we proceed as follows. Assuming the total electrostatic interaction to be a pair potential and requiring that $\Delta E_{\rm AS} = 0$ in a perfect fcc lattice including only nearest neighbors it is possible to write[2]

$$\Delta E_{\rm AS}^{\rm MM} = \alpha \sum_i \left[\bar{n}_i - \frac{n_0}{12} \sum_{j \neq i} e^{-\eta(r_{ij}/\beta - s_0)} \right] . \tag{A5}$$

If the atoms considered are different, we restrict ourselves to the region of positive overlap and estimate[7,5]

$$\Delta E_{\rm AS}^{\rm AM} = -\int_{\text{overlap region}} d\mathbf{r} [\Delta n^M(\mathbf{r}) \Delta\Phi^A(\mathbf{r}) + \Delta n^A(\mathbf{r}) \Delta\Phi^M(\mathbf{r})] , \tag{A6}$$

where M and A means metal and adsorbate atom, respectively, and Φ is the electrostatic potential originating from the respective atom. The inclusion of the overlap region and neglect of the "holes" normally results in an overestimate of the repulsion.

The atomic sphere correction between two Pd atoms is taken from (A5), while the correction between Pd and H atoms i and k from (A6) is described in a form

$$\Delta E_{{\rm AS},ik}^{\rm H,Pd} = V^{\rm H,Pd} \Omega_{ik} e^{-\phi_M^{\rm H,Pd} s_i - \phi_A^{\rm H,Pd} s_k - \phi_R^{\rm H,Pd} r_{ik}} , \tag{A7}$$

where the prefactor $\Omega_{ik}(s_i, s_k, r_{ij})$ is the overlap volume of the two neutral spheres.

In most of our calculations the correction term $\Delta E_{\rm 1el}$ has been put equal to the constant -0.27 eV per hydrogen atom until the Pd d band is filled when the number of atoms of the two kinds become equal. At higher θ we assume a filled d band and thus no change in $\Delta E_{\rm 1el}$ since $\theta = 1$, in other words $\Delta E_{\rm 1el} = -0.27$ eV per palladium atom.

As the density contribution from one hydrogen atom to another is normally negligible compared to the contribution from the metal, it is neglected in the calculation of the neutral radius s of a hydrogen atom. Thus we have the relations (indices i and j refer to Pd atoms, k and l to H):

$$\begin{aligned}
&\bar{n}_i^{\rm Pd} = n_0^{\rm Pd} \exp[-\eta^{\rm Pd}(s_i - s_0^{\rm Pd})] \\
&\quad = \sum_{\rm Pd} \frac{n_0^{\rm Pd}}{12} \exp[\eta_1^{\rm Pd}(s_i - s_0^{\rm Pd}) - \eta_2^{\rm Pd}(r_{ij} - \beta s_0^{\rm Pd})] + \sum_{\rm H} \tilde{n}_0^{\rm H} \exp[\tilde{n}_1^{\rm H}(s_i - \tilde{s}_0^{\rm H}) - \tilde{\eta}_2^{\rm H}(r_{ij} - \tilde{r}_0^{\rm H})] , \\
&\bar{n}_k^{\rm H} - \sum_{\rm H} \frac{n_0^{\rm H}}{12} \exp[-\eta_2^{\rm H}(r_{kl} - \beta s_0^{\rm H})] = n_0^{\rm H} \exp[-\eta^{\rm H}(s_k - s_0^{\rm H})] = \sum_{\rm Pd} \tilde{n}_0^{\rm Pd} \exp[\tilde{\eta}_1^{\rm Pd}(s_k - \tilde{s}_0^{\rm Pd}) - \tilde{\eta}_2^{\rm Pd}(r_{kj} - \tilde{r}_0^{\rm Pd})] , \\
&E_{c,i}^{\rm Pd} = E_0^{\rm Pd} + E_2^{\rm Pd} \left[\frac{\bar{n}_i^{\rm Pd}}{n_0^{\rm Pd}} - 1 \right]^2 + E_3^{\rm Pd} \left[\frac{\bar{n}_i^{\rm Pd}}{n_0^{\rm Pd}} - 1 \right]^3 , \\
&E_{c,k}^{\rm H} = E_0^{\rm H} + E_2^{\rm H} \left[\frac{\bar{n}_k^{\rm H}}{n_0^{\rm H}} - 1 \right]^2 + E_3^{\rm H} \left[\frac{\bar{n}_k^{\rm H}}{n_0^{\rm H}} - 1 \right]^3 , \\
&\Delta E_{\rm AS} = \sum_{\rm Pd} \left[\alpha^{\rm Pd} \left[\bar{n}_i - \frac{1}{12} \sum_{\rm Pd} \exp[-\eta^{\rm Pd}(r_{ij}/\beta - s_0^{\rm Pd})] \right] + \sum_{\rm H} V^{\rm H,Pd} \Omega_{ij} \exp[-\phi_M^{\rm H,Pd} s_i - \phi_A^{\rm H,Pd} s_k - \phi_R^{\rm H,Pd} r_{ik}] \right] , \\
&E_{\rm tot} = \sum_{\rm Pd} E_{c,i}^{\rm Pd} + \sum_{\rm H} E_{c,k}^{\rm H} + \Delta E_{\rm AS} + \sum_{\rm H} \Delta E_{\rm 1el} + \sum_{\rm H\ pairs} \delta(r_{kl}) .
\end{aligned} \tag{A8}$$

TABLE I. EMT parameters. The values in parentheses refer to diffusion barrier calculations; the values correspond to a considerable softening of the potential from $\Delta E_{AS}^{H,Pd}$ and a reduction of the strength of this term of 40% in the ground state, see Sec. III C.

Atom	H	Pd	Ni	Pt
E_0	−2.14	−4.67	−5.12	−4.92
E_2	0.284	2.20	2.14	2.18
E_3	−0.11	−0.59	−1.04	−0.60
n_0	0.007 76	0.012 28	0.0150	0.0116
s_0	1.71	2.873	2.599	2.894
η	4.1	1.965	1.93	2.54
η_1	3.2	0.164	0.37	0.11
$\tilde{n}_0$	0.001 19	0.007 86	0.005 17	0.009 75
$\tilde{s}_0$	2.8	1.8	1.8	1.8
$\tilde{r}_0$	3.5	3.5	3.5	3.5
$\tilde{\eta}_1$	1.33	0.78	0.53	0.80
$\tilde{\eta}_2$	2.26	1.96	1.74	1.98
α		2400	1440	3170
$V^{H,M}$		26 800 (9.945)	1860	23 900
$\phi_M^{H,M}$		1.24(1.20)	0.74	1.21
$\phi_A^{H,M}$		1.83(1.10)	1.54	1.73
$\phi_R^{H,M}$		1.93(0.065)	1.83	1.87

From the first two equations the neutral radii are calculated. In the case of Pd it has to be done iteratively. Now the densities and then all the rest is calculated straightforwardly.

The parameters η and η_1 are closely connected to the bulk and shear moduli of the metal. From calculations of Pd in a homogeneous electron gas a value of s_0 is found which is 6% lower than the experimental value. The bulk modulus calculated is about two times the experimental value. This is due to d—d bonding which is not included in the calculations. To get an accurate description of the bulk metal we fit the parameters s_0^{Pd} and η^{Pd} to these two measured quantities. The parameter η_1^{Pd} is determined from the experimental shear modulus as is usually necessary. All other parameters are derived from LDA calculations of the metal in jellium. The same fitting procedure has been applied to Ni and Pt. Values of the parameters described above may be found in Table I.

APPENDIX B: FITTING PROCEDURE FOR $\Delta E_{AS}^{H,Pd}$

The fitting of $\Delta E_{AS}^{H,Pd}$ has been done in the following way. We want to optimally describe the situation on top of the diffusion barrier, where a hydrogen atom is much closer to the palladium atoms than in the interstitial sites. Therefore, we first determine the four parameters entering (A7) by interpolating a number of H/Je calculations corresponding to a new density regime including the values at the energy maximum. This procedure changes all parameters but does not involve any fitting.

The parameter determining the "softness" of $\Delta E_{AS}^{H,Pd}$ is obviously ϕ_R. When we change this we also have to change $V^{H,Pd}$, which includes terms of the form $\exp[\phi_M^{H,Pd}s_0^{Pd}+\phi_A^{H,Pd}s_0^{H}+\phi_R^{H,Pd}r_0]$. Unfortunately, it is not so simple that we can just adjust the prefactor to give the same magnitude of $\Delta E_{AS}^{H,Pd}$ in the ground state as before the fitting. This is due to the fact that lattice relaxations change with ϕ_R, thus changing several different contributions to the total energy.

Thus we now fit the two parameters $V^{H,Pd}$ and ϕ_R to reproduce the total energy of the ground state as calculated with the original $\Delta E_{AS}^{H,Pd}$ and to give the experimental value of the ground-state vibrational frequency of H at the octahedral site of Pd (Table I). The unit cell used contains $3\times3\times3$ primitive unit cells as usual. The resulting softening changing ϕ_R from 1.8 to 0.065 is reflected in the change of ω_0 from 126 to 67.5 meV, within 2% of the experimental value.[1] The change of $V^{H,Pd}$ from 4700 to 9.945 corresponds to an increase of $\Delta E_{AS}^{H,Pd}$ from 205 to 281 meV, which is compensated by other terms in the total energy as the local distortion of the lattice is less when $\Delta E_{AS}^{H,Pd}$ is softer.

[1]E. Wicke and H. Brodowsky, *Hydrogen in Palladium and Palladium Alloys in Hydrogen in Metals II*, Vol. 29 of *Topics in Applied Physics* edited by G. Alefeld and J. Völkl (Springer, Berlin 1978), p. 73 and references therein.

[2]K. W. Jacobsen, J. K. Nørskov, and M. J. Puska, Phys. Rev. B **35**, 7423 (1987); K. W. Jacobsen, Comments Condens. Matter Phys. **14**, 129 (1988).

[3]J. K. Nørskov and F. Besenbacher, J. Less Common Met. **130**, 475 (1987).

[4]J. K. Nørskov and N. D. Lang, Phys. Rev. B **21**, 2136 (1980). J. K. Nørskov, *ibid.* **26**, 2875 (1982).

[5]J. K. Nørskov, J. Chem. Phys. **90**, 7461 (1989).

[6]J. K. Nørskov and K. W. Jacobsen, in *The Structure of Surfaces II*, Vol. 11 of *Springer Series in Surface Sciences*, edited by J. F. van der Veen and M. A. van Hove (Springer, Berlin, 1987), p. 118.

[7]K. W. Jacobsen and J. K. Nørskov, Phys. Rev. Lett. **59**, 2764 (1987); **60**, 2496 (1988).

[8]P. Stoltze, K. W. Jacobsen, and J. K. Nøskov, Phys. Rev. B **36**, 5035 (1987); P. Stoltze, J. K. Nørskov, and U. Landman, Phys. Rev. Lett. **61**, 440 (1988).

[9]M. S. Daw and M. I. Baskes, Phys. Rev. B **29**, 6443 (1984); S. M. Foiles and M. S. Daw, J. Vac. Sci. Technol. A **3**, 1565 (1985).

[10]L. R. Pratt and J. Eckert, Phys. Rev. B **39**, 13 171 (1989).

[11]O. B. Christensen, P. D. Ditlevsen, K. W. Jacobsen, P. Stoltze, O. H. Nielsen, and J. K. Nørskov, Phys. Rev. B **40**, 1993 (1989).

[12]M. J. Stott and E. Zaremba, Phys. Rev. B **22**, 1564 (1980).

[13]P. Hohenberg and W. Kohn, Phys. Rev. **136**, B864 (1964); W. Kohn and L. J. Sham, Phys. Rev. **140**, A1133 (1965).

[14]D. M. Newns, Phys. Rev. **178**, 1123 (1969).

[15]J. K. Nørskov, Phys. Rev. B **20**, 446 (1979).

[16]W. H. Press, B. P. Flannery, S. A. Teukolsky, and W. T. Vetterling, *Numerical Recipes* (Cambridge University Press, London, 1986).

[17]W. H. Mueller, J. P. Blackledge, and G. G. Libowitz, *Metal Hydrides* (Academic, New York, 1968).

[18]J. E. Schirber and B. Morosin, Phys. Rev. B **12**, 117 (1975).

[19]R. Feenstra, Ph.D. thesis, Vrije Universiteit, Amsterdam, 1985.

[20]S.-H. Wei and A. Zunger (unpublished).

[21]J. Völkl and G. Alefeld, *Diffusion of Hydrogen in Metals in Hydrogen in Metals I,* Vol. 28 of *Topics in Applied Physics,* edited by G. Alefeld and J. Völkl (Springer, Berlin, 1978), p. 321.

[22]O. K. Andersen, O. Jepsen, and D. Glötzel, *Canonical Description of the Band Structures of Metals,* in *Highlights of Condensed-Matter Theory,* LXXXIX Corso Soc. Italiana di Fisica (Tipografia Compositori, Bologna, 1985).